

Berkeley Feb 23 1994

A CsI calorimeter for γ -ray space experiments

P. Carlson, C. Fuglesang* and P. Persson
Royal Inst of Technology, Stockholm

* European Astronaut
Center, Köln.

Scientific goals : structures in γ -ray
energy distributions,
point sources and
diffuse radiation

Design aim : • Improve $\frac{\Delta E}{E}$ over existing
detectors (e.g. ECRIF)
by an order of magnitude,
• Optimize angular resolution

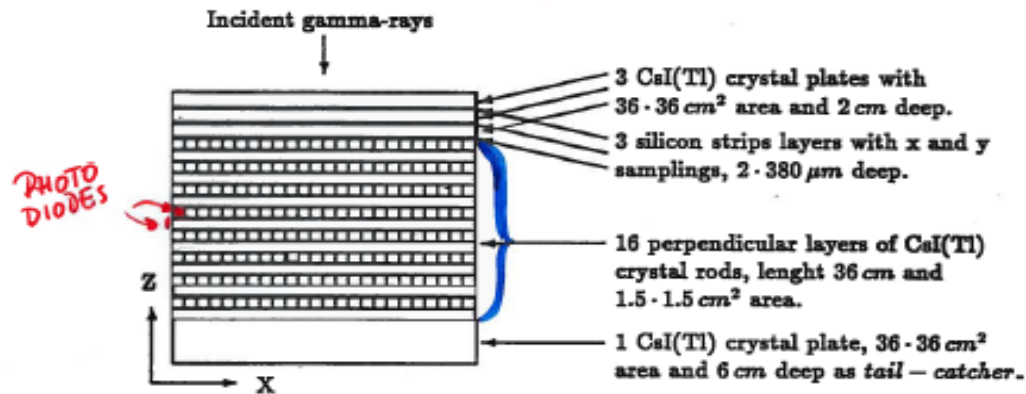


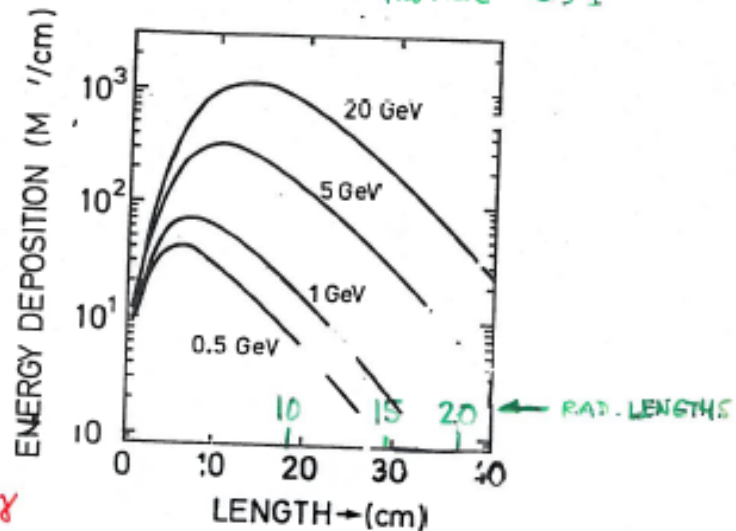
Figure 7.1: Geometrical setup for the final calorimeter prototype.

- Total area: 1300 cm^2
- Depth: 36 cm (19 x₀)
- Readout: photo diodes

3 plates	2cm		6cm
16 layers, 24 rods	1.5cm		24cm
1 plate	6cm		6cm
Total			36 cm
			(19.5 rod length)

Area $36 \times 36 \text{ cm}^2 = 1296 \text{ cm}^2$, 211 kg CsI
 $50 \times 50 \text{ cm}^2 = 2500 \text{ cm}^2$, 408 kg CsI

LONGITUDINAL PROFILE CsI



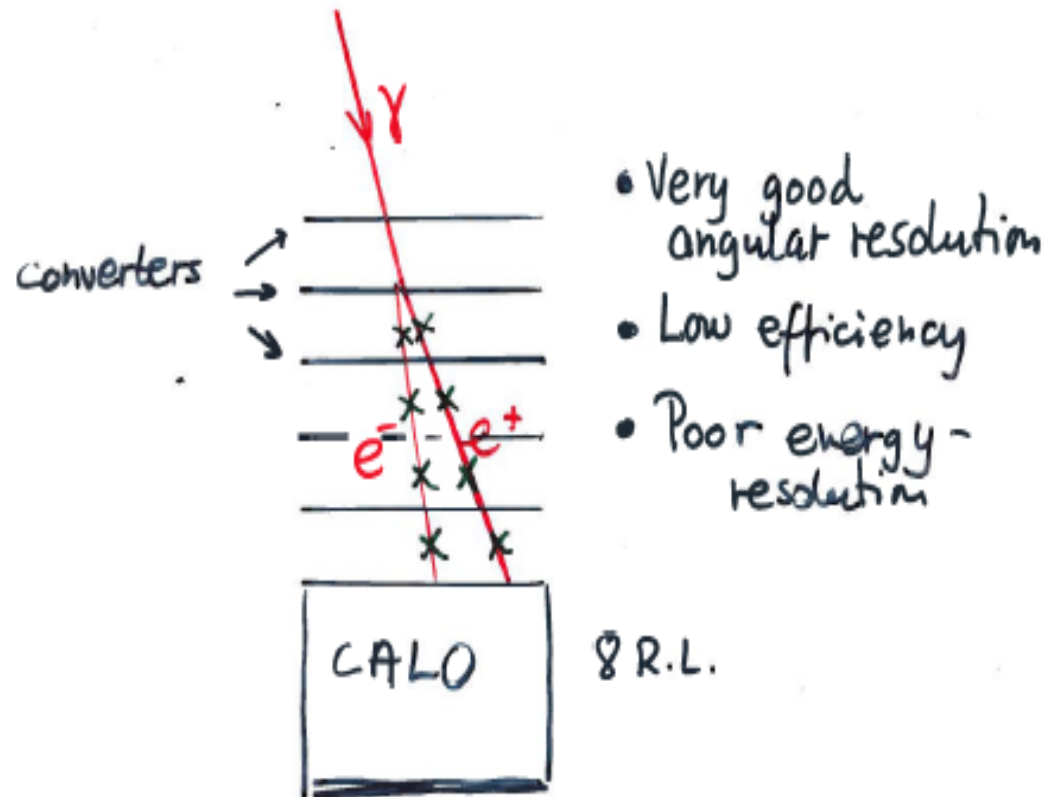
TRANSVERSE PROFILE :

UP TO SHOWER MAX : $r < 1 X_0$ (1.9cm CsI)

AFTER SHOWER MAX : 90% $r < r_M$ (Molière radius) (3.8cm)

- POSITION OF SHOWER MAX. $\propto \lg(E)$
- 1 GeV GIVES $3 \cdot 10^6$ PHOTO ELECTRONS IN A DIODE - LARGE SIGNAL !!
- LEAKAGE INCREASES WITH E_T

Existing γ -ray detectors



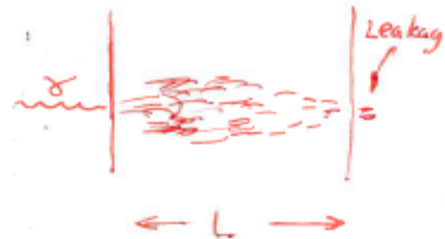
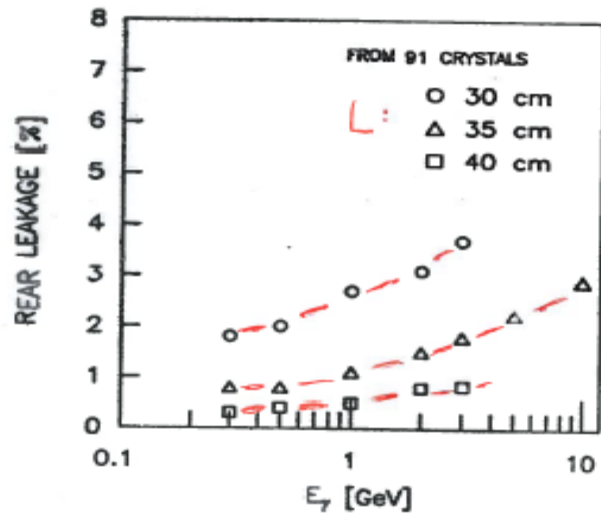
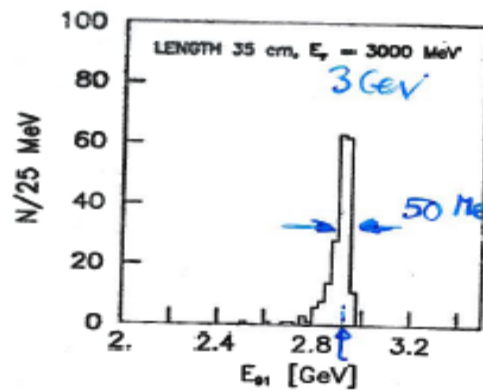


Figure 3. Rear leakage as function of photon energy for different depths of Cal(Tl).

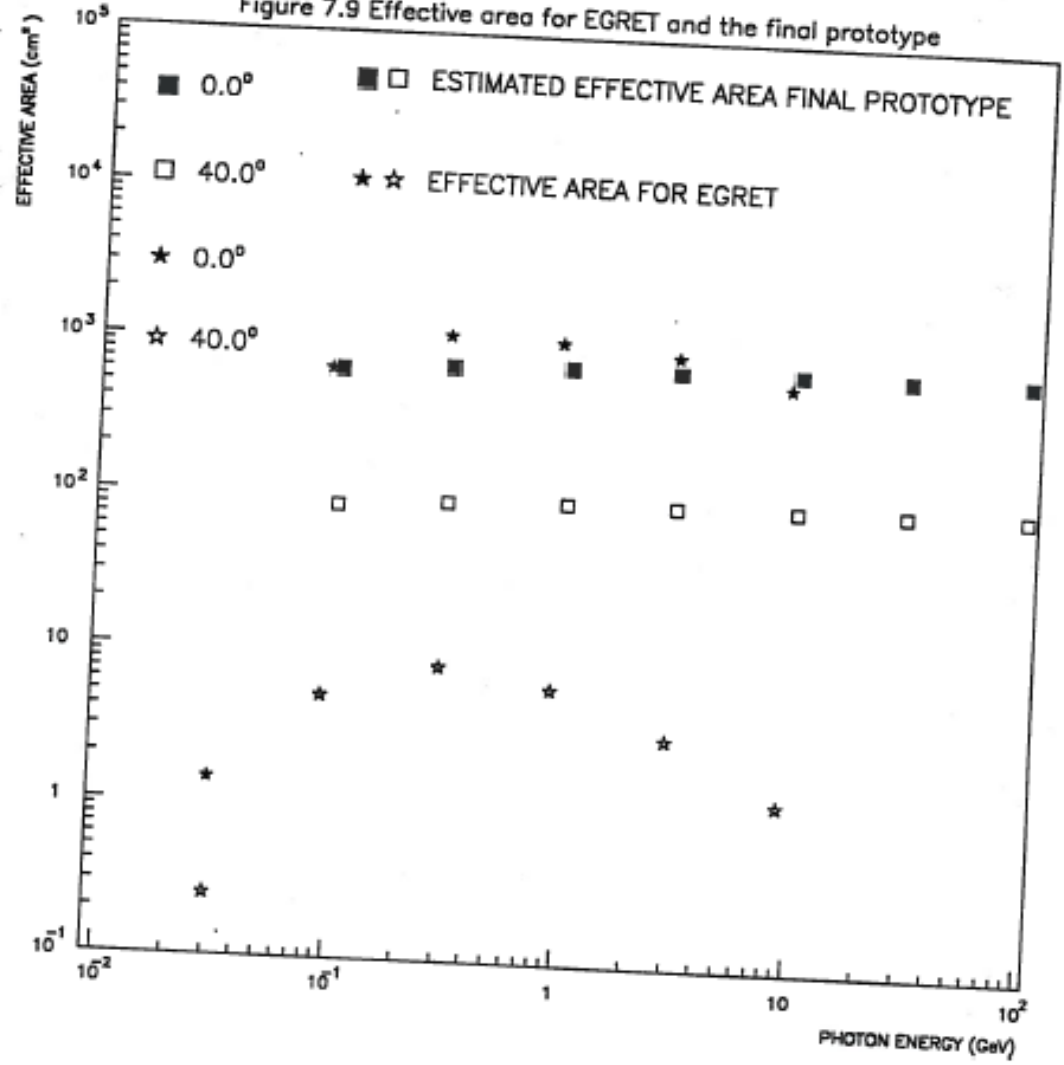


ENERGIUPPLÖSNING
 (SIMULERINGSRESULTAT)

RMS UPPL. $\pm 0.7\%$

Figure 4. Energy deposit in 35 cm Cal(Tl) for 3 GeV gamma-ray energy.

Figure 7.9 Effective area for EGRET and the final prototype



1 GeV CsI

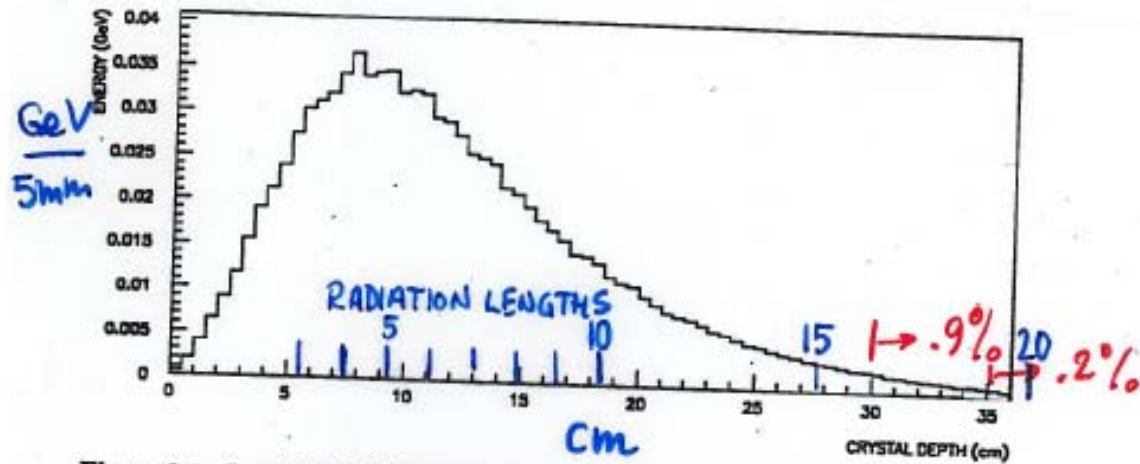


Figure 2.1: Longitudinal development of an electromagnetic shower with an incident photon energy of $E_0 = 1 \text{ GeV}$ in a CsI(Tl) calorimeter from Monte Carlo simulations. Energy deposition per 5 mm CsI(Tl) crystal is shown as a function of crystal depth.

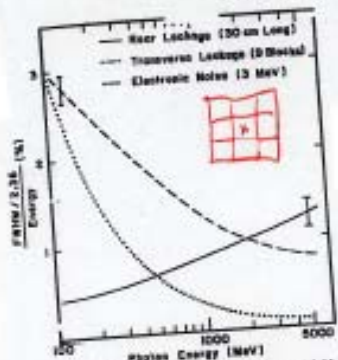


Fig. 3. Contribution to energy resolution in CsI blocks attributable to the three dominant sources: rear leakage from 30 cm long crystals, transverse leakage from nine square crystals 5 cm on a side, and electronic noise, assumed to be 3 MeV. The error bars show typical uncertainties in the curves.

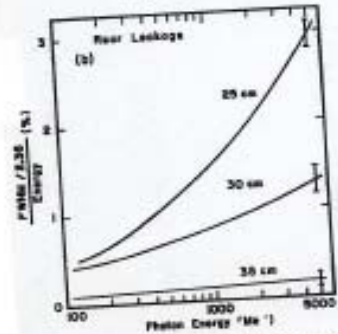
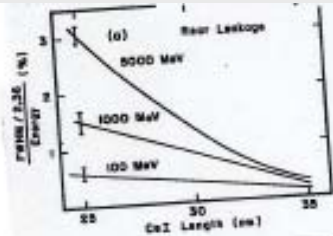


Fig. 4. The RGS prediction for the fluctuation in energy loss from rear leakage in CsI crystals vs (a) length of the crystals, and (b) incident photon energy. The error bars show typical uncertainties in the curves.

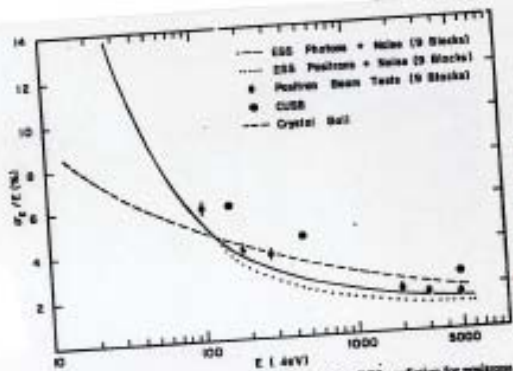
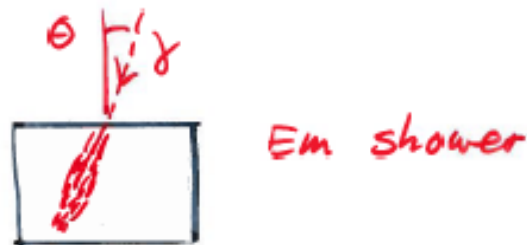


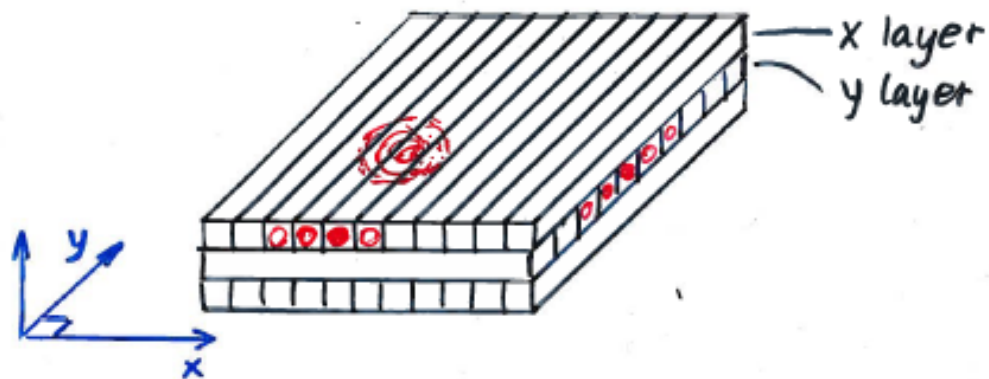
Fig. 5. Energy resolution as a function of energy, showing the RGS prediction for positrons and photons incident on 5 cm by 5 cm by 30 cm CsI crystals from the sum of nine blocks. No effects from nonzero light collection gradients or material between or in front of the crystals are included in the predictions. Also plotted are the positron test beam results on CsI reported here, as well as the Crystal Ball [16] and CUSS [11] resolutions.

SIMULATION STUDY OF AN ELECTROMAGNETIC CALORIMETER OF CsI (TE)

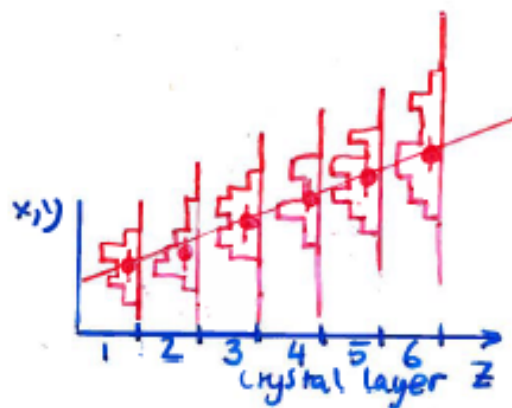
- CsI well established as E-M calorimeters in particle physics experiments, e.g. CERN, CORNELL
- Energy resolution superb and well known
- Directional properties not studied



optimize determination of θ !

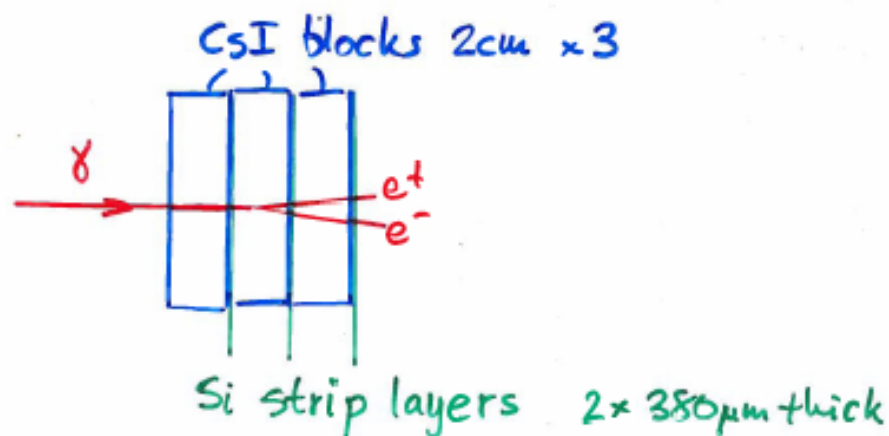


CsI crystals $1.5 \times 1.5 \text{ cm}^2$
 smallest cross-section that we can handle



TO IMPROVE ANGULAR RESOLUTION

MEASURE FIRST e^+e^- PAIR



50% convert in 2cm

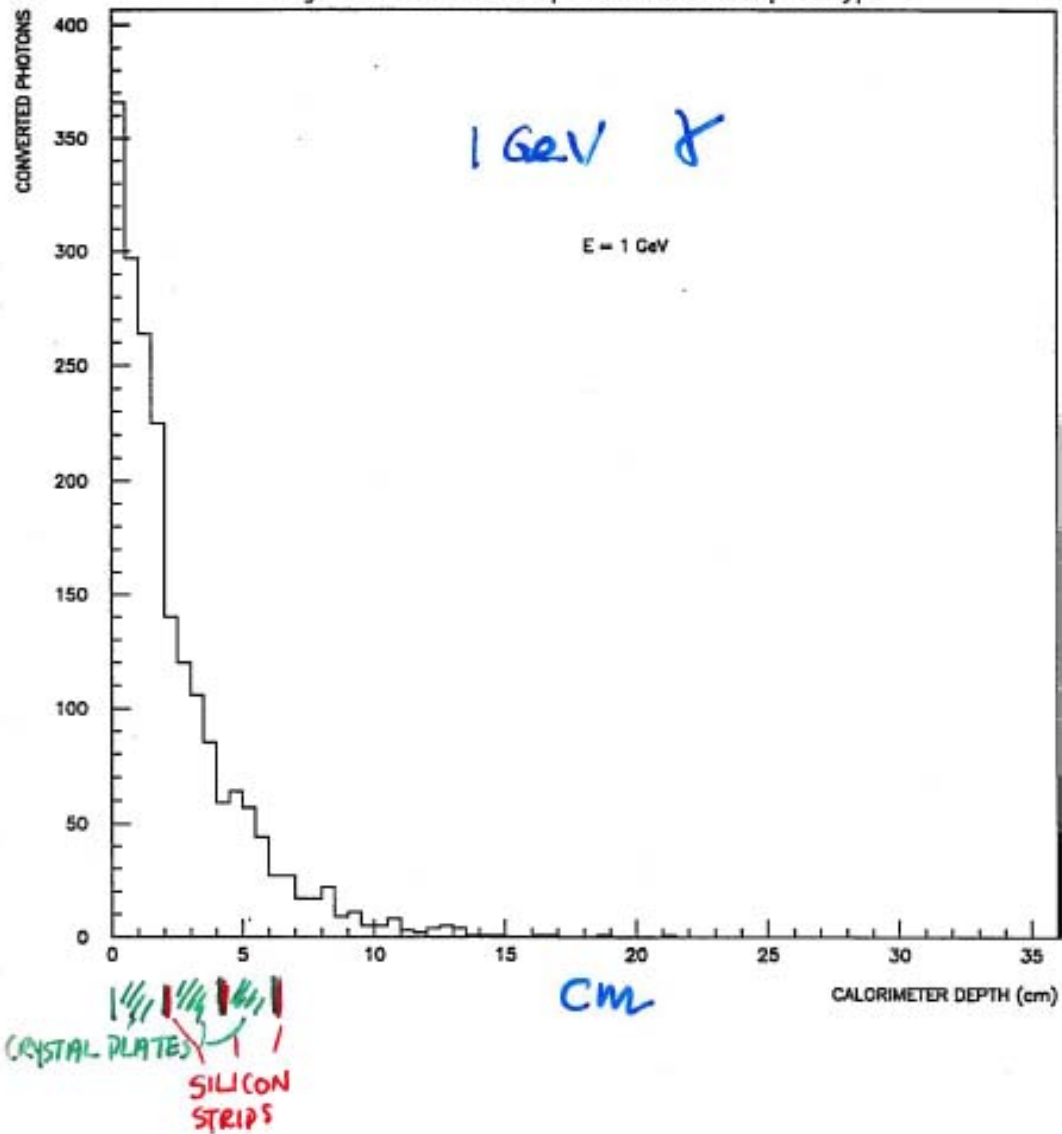
80% 4cm

90% 6cm

"Trigger efficiency" 90% 3 Si layers

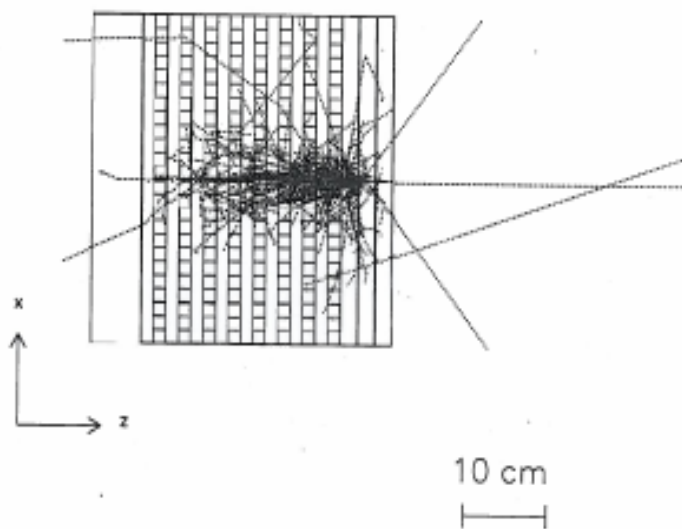
PHOTON CONVERSION POINT

Figure 7.2 Conversion points in the final prototype



A simulated electromagnetic shower

3/2/94



Incident photon energy [GeV]	0.100	0.300	1.000	3.000	10.00	30.00	100.0
Simulated energy resolution [%]	0.47	1.36	1.14	0.96	0.68	0.77	0.90
Material inhomogeneities and calibration errors [%]	1.0	1.0	1.0	1.0	1.0	1.0	1.0
Electronic read - out noise [%]	4.40	1.47	0.44	0.15	0.05	0.02	0.01
Estimated energy resolution [%]	4.54	2.24	1.58	1.40	1.21	1.27	1.35

Table 7.6: Estimated contributions to the total energy resolution and the resulting estimated energy resolution versus the incident photon energy for the final calorimeter prototype.

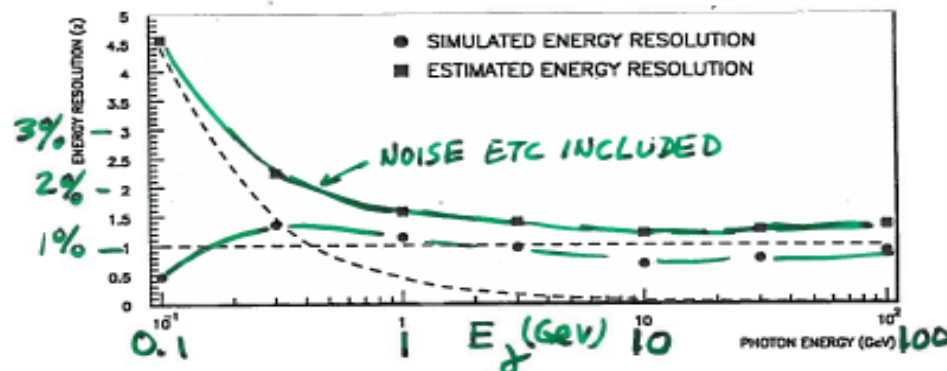


Figure 7.8: The simulated energy resolution, the estimated contributions to the total energy resolution as dashed lines, and the resulting energy resolution as functions of the incident photon energy for the final calorimeter prototype.

7.6 Estimated effective area

The effective area is derived for the calorimeter on the basis of the following expression

$$\text{Effective area} = \text{Efficiency} \cdot \text{Acceptance area} [\text{cm}^2] \quad (7.2)$$

where the acceptance area is estimated from the assumptions that along the shower axis, a cylinder with a radius of one Moliere radius (3.8 cm) and a length of about 19 radiation lengths (35.5 cm) should always be available. These assumptions lead to the following expression for the acceptance area

$$\text{Acceptance area} = (28.4 - 35.5 \cdot \sin \alpha) \cdot (28.4 - 35.5 \cdot \sin \beta) [\text{cm}^2] \quad (7.3)$$

where α and β are the angles of incidence for each measurement plane. The angle θ between the incident gamma-ray trajectory and the normal to the calorimeter is

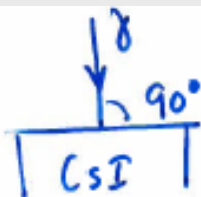


Figure A.10 Distribution of angles for the final prototype

